



2009

Stem Cells from Deciduous Tooth Repair Mandibular Defect in Swine

Y Zheng

Y Liu

C M. Zhang


W H. Li

S Shi

University of Pennsylvania

See next page for additional authors

Follow this and additional works at: https://repository.upenn.edu/dental_papers

 Part of the [Endodontics and Endodontology Commons](#), [Oral and Maxillofacial Surgery Commons](#), [Oral Biology and Oral Pathology Commons](#), and the [Periodontics and Periodontology Commons](#)

Recommended Citation

Zheng, Y., Liu, Y., Zhang, C. M., Li, W. H., Shi, S., Le, A. D., & Wang, S. L. (2009). Stem Cells from Deciduous Tooth Repair Mandibular Defect in Swine. *Journal of Dental Research*, 88 (3), 249-254. <http://dx.doi.org/10.1177/0022034509333804>

At the time of publication, author Shihong Shi was affiliated with the University of Southern California, School of Dentistry. Currently, (s)he is a faculty member at the School of Dental Medicine at the University of Pennsylvania. At the time of publication, author Anh D. Le was affiliated with the University of Southern California, School of Dentistry. Currently, (s)he is a faculty member at the School of Dental Medicine at the University of Pennsylvania.

This paper is posted at ScholarlyCommons. https://repository.upenn.edu/dental_papers/463
For more information, please contact repository@pobox.upenn.edu.

Stem Cells from Deciduous Tooth Repair Mandibular Defect in Swine

Abstract

Stem cells from human exfoliated deciduous teeth have been identified as a new post-natal stem cell population with multipotential differentiation capabilities, including regeneration of mineralized tissues in vivo. To examine the efficacy of utilizing these stem cells in regenerating orofacial bone defects, we isolated stem cells from miniature pig deciduous teeth and engrafted the critical-size bone defects generated in swine mandible models. Our results indicated that stem cells from miniature pig deciduous teeth, an autologous and easily accessible stem cell source, were able to engraft and regenerate bone to repair critical-size mandibular defects at 6 months post-surgical reconstruction. This pre-clinical study in a large-animal model, specifically swine, allows for testing of a stem cells/scaffold construct in the restoration of orofacial skeletal defects and provides rapid translation of stem-cell-based therapy in orofacial reconstruction in human clinical trials.

Keywords

Author keywords: Bone, Deciduous tooth, Miniature pig, Stem cell, Tissue engineering MeSH: Animals, Bone Regeneration, Cells, Cultured, Dental Pulp, Disease Models, Animal, Feasibility Studies, Female, Green Fluorescent Proteins, Guided Tissue Regeneration, Mandibular Diseases, Microscopy, Fluorescence, Osteogenesis, Reconstructive Surgical Procedures, Stem Cell Transplantation, Stem Cells, Swine, Swine, Miniature, Tissue Engineering, Tissue Scaffolds, Tomography, X-Ray Computed, Tooth, Deciduous, Transplantation, Autologous Emtree drug terms: diagnostic agent, green fluorescent protein, tissue scaffold Emtree medical terms: animal, article, autotransplantation, bone development, bone regeneration, cell culture, computer assisted tomography, cytology, deciduous tooth, disease model, feasibility study, female, fluorescence microscopy, jaw disease, methodology, minipig, physiology, plastic surgery, stem cell, stem cell transplantation, swine, tissue engineering, tissue regeneration, tooth pulp

Disciplines

Dentistry | Endodontics and Endodontology | Oral and Maxillofacial Surgery | Oral Biology and Oral Pathology | Periodontics and Periodontology

Comments

At the time of publication, author Shihong Shi was affiliated with the University of Southern California, School of Dentistry. Currently, (s)he is a faculty member at the School of Dental Medicine at the University of Pennsylvania.

At the time of publication, author Anh D. Le was affiliated with the University of Southern California, School of Dentistry. Currently, (s)he is a faculty member at the School of Dental Medicine at the University of Pennsylvania.

Author(s)

Y Zheng, Y Liu, C M. Zhang, W H. Li, S Shi, A D. Le, and S L. Wang

Y. Zheng¹, Y. Liu¹, C.M. Zhang¹, H.Y. Zhang², W.H. Li², S. Shi³, A.D. Le^{3*}, and S.L. Wang^{1,4*}

¹Salivary Gland Disease Center and the Molecular Laboratory for Gene Therapy & Tooth Regeneration, Capital Medical University School of Stomatology, Tian Tan Xi Li No.4, Beijing 100050, China; ²Department of Cell Biology, Municipal Laboratory for Liver Protection and Regulation of Regeneration, Capital Medical University School of Basic Medical Sciences, You An Men Wai No.10, Beijing 100069, China; ³The Center for Craniofacial Molecular Biology, University of Southern California School of Dentistry, 2250 Alcazar Street, CSA 103, Los Angeles, CA 90033, USA; and ⁴Department of Biochemistry and Molecular Biology, Capital Medical University School of Basic Medical Sciences, You An Men Wai No.10, Beijing 100069, China; *corresponding authors, slwang@ccmu.edu.cn and anhle@usc.edu

J Dent Res 88(3):249-254, 2009

ABSTRACT

Stem cells from human exfoliated deciduous teeth have been identified as a new post-natal stem cell population with multipotential differentiation capabilities, including regeneration of mineralized tissues *in vivo*. To examine the efficacy of utilizing these stem cells in regenerating orofacial bone defects, we isolated stem cells from miniature pig deciduous teeth and engrafted the critical-size bone defects generated in swine mandible models. Our results indicated that stem cells from miniature pig deciduous teeth, an autologous and easily accessible stem cell source, were able to engraft and regenerate bone to repair critical-size mandibular defects at 6 months post-surgical reconstruction. This pre-clinical study in a large-animal model, specifically swine, allows for testing of a stem cells/scaffold construct in the restoration of orofacial skeletal defects and provides rapid translation of stem-cell-based therapy in orofacial reconstruction in human clinical trials.

KEY WORDS: deciduous tooth, stem cell, bone, tissue engineering, miniature pig

DOI: 10.1177/0022034509333804

Received April 19, 2008; Last revision January 6, 2009; Accepted January 30, 2009

A supplemental appendix to this article is published electronically at <http://jdr.sagepub.com/supplemental>.

Stem Cells from Deciduous Tooth Repair Mandibular Defect in Swine

INTRODUCTION

Reconstruction of orofacial defects secondary to tumors and trauma relies on different sources of bone grafts with inherent morbidity. Stem-cell-based tissue engineering is a promising alternative for bone regeneration (Petite *et al.*, 2000; Bianco *et al.*, 2001; Rose and Oreffo, 2002). The stem-cell-based therapeutic approach can restore bone defects without incurring graft donor site morbidity. Bone marrow mesenchymal stem cells (BMMSCs) have emerged as an important cell source for bone regeneration (Gronthos *et al.*, 2003; Mankani *et al.*, 2006; Mastrogiacomo *et al.*, 2007), as has been demonstrated clinically in femur fracture repair and regeneration (Shao *et al.*, 2006). Previous studies have indicated that the orofacial bone and dental tissues contain a variety of stem cells, including dental pulp stem cells (DPSCs), stem cells from human exfoliated deciduous teeth (SHED), periodontal ligament stem cells (PDLSCs), and orofacial mesenchymal stem cells (Akintoye *et al.*, 2006). These orofacial stem cells possess a higher proliferation capacity when compared with BMMSCs, and their origin may be associated with neural crest cells (Gronthos *et al.*, 2000; Shi *et al.*, 2002; Shi and Gronthos, 2003; Seo *et al.*, 2004; Akintoye *et al.*, 2006). When transplanted subcutaneously into immunocompromised mice, SHEDs, an easily accessible stem cell source, are capable of generating robust amounts of bone *in vivo* (Miura *et al.*, 2003; Seo *et al.*, 2008), suggesting a potential for bone regeneration. To explore the feasibility of using SHED-based bone regeneration to treat orofacial bone defects, we utilized swine as a pre-clinical animal model to test the regeneration of critical-size mandibular defects using SHEDs. Our previous studies demonstrated that miniature pigs (minipig) are appropriate large-animal models for oral and craniofacial tissue engineering and therapies (Shan *et al.*, 2005; Sonoyama *et al.*, 2006; Wang *et al.*, 2007; Yan *et al.*, 2007; Liu *et al.*, 2008). In this study, we utilized minipigs as a large-animal model to examine the feasibility of using autologous stem cells derived from miniature pig deciduous teeth—that is, SPD—to repair critical-size mandibular bone defects.

MATERIALS & METHODS

Animals

Sixteen inbred female minipigs (4–6 mos old, weighing 20–30 kg each) were obtained from the Institute of Animal Science of the Chinese Agriculture University. Minipigs were kept under conventional conditions, with free access to water and a regular supply of soft food diet. The study was performed in accordance with a protocol approved by the Animal Care and Use Committees of Capital Medical University.

Cell Culture

Deciduous incisor pulp tissues from first and second deciduous incisors were harvested from 16 inbred female minipigs. SPDs were isolated and cloned following established

protocols (Gronthos *et al.*, 2000; Miura *et al.*, 2003; Seo *et al.*, 2008; Appendix).

Immunocytochemistry

SPDs were subcultured in 24-chamber slides. Cells were fixed in 4% paraformaldehyde for 15 min, blocked with non-specific antibodies, and incubated with either anti-STRO-1 (R&D, Minneapolis, MN, USA) at dilutions of 1:200 to 1:500 or anti-vimentin (Chemicon, Temecula, CA, USA) at a dilution of 1:500 for 1 hr according to the manufacturer's protocol. To test mouse anti-human STRO-1 antibody cross-reactivity with pig tissues, we performed immunocytochemical stain on human SHEDs, minipig SPDs, and lymphocytes, and found that only human SHEDs and pig SPDs were specifically stained with human STRO-1 antibody. Based on these findings, we utilized mouse anti-human monoclonal antibody to STRO-1 in this study. Samples were subsequently incubated with goat secondary antibodies for 45 min, and observed by fluorescence microscopy. Non-immune serum served as negative control. Subsequently, sections were counterstained with DAPI. We used an alkaline phosphatase detection kit (Chemicon) to examine the expression of ALP according to the manufacturer's protocol, and the result was observed by light microscopy.

Flow Cytometric Analysis

Detached cells were permeabilized with PBS containing 0.1% (wt/v) saponin at room temperature for 20 min. After being blocked with normal serum, the cells were incubated with fluorescein isothiocyanate (FITC)-conjugated STRO-1 antibodies (R&D Systems; clone STRO-1) or phycoerythrin (PE)-conjugated ALP antibodies (R&D systems; clone B4-78) for 30 min at room temperature. After 3 washes with PBS containing 0.1% saponin, fluorescence was analyzed by a FACSCalibur flow cytometer with CellQuest software (BD Bioscience, Palo Alto, CA, USA). Positive cells were identified by comparison with the corresponding isotype controls (FITC- or PE-conjugated IgG) in which a false-positive rate of less than 2% was accepted.

Transfection of eGFP Genes

Conditional retroviral supernatants were produced by the stable retrovirus-producing cell lines PT67/eGFP as described previously (Brazelton and Blau, 2005; Zhang *et al.*, 2005). For transfection, about 1×10^5 SPD grown in 6-well plates were incubated for approximately 20 hrs with a mixture of 1 vol of viral supernatant and growth medium at equal vols and in the presence of 8 $\mu\text{g}/\text{mL}$ polybrene (Sigma, St. Louis, MO, USA). A repeated transfection was performed in a period of 72 hrs, and the transfected cultures were selected with G418 (100 $\mu\text{g}/\text{mL}$, Sigma). The transfection efficiency of the cells was 80%.

Scanning Electron Microscopy

GFP-positive SPDs were grown on β -TCP carrier (Biomedical Materials and Engineering Center of Wuhan University of Technology, China) for 7 days and fixed with 2.5% glutaraldehyde in 0.1 M sodium cacodylate buffer (pH 7.2) for 2 hrs at 4°C. The samples were examined under a Hitachi S-520 scanning electron microscope (Hitachi, Tokyo, Japan; <http://www.hitachi.com/>).

Reconstruction of Mandibular Bone Defects in Swine Model with SPDs

A critical-size defect of $2.5 \times 1.5 \times 1.5 \text{ cm}^3$ was surgically created in the parasymphiseal region of the mandible in 10 minipigs for a long-term

(24 wks) follow-up so that we could evaluate bone regeneration (Henkel *et al.*, 2005). In another 6 minipigs, we created 2 smaller defects of $1.0 \times 1.0 \times 0.5 \text{ cm}^3$ bilaterally in the parasymphysis of the mandible and evaluated short-term post-surgical follow-ups, at 2 wks ($n = 3$) and 4 wks ($n = 3$) (Appendix Fig. 1).

Computed Tomography (CT) Assessment of Bone Formation

CT imaging of the minipig's mandible (Siemens Company, Bensheim, Germany) was carried out at 2, 4, 12, and 24 wks after transplantation at a scanning length of 0.75 mm.

Quantitative and Histological Evaluation of Regenerated Bone

Bone specimens were fixed in 10% buffered formalin. Half of the specimens were decalcified and embedded in paraffin, while the other half were processed as non-decalcified. Sections of 5- to 6- μm thickness from the embedded specimen were stained with H&E. The extent of ossification within each section was analyzed semi-quantitatively by histomorphometric techniques (Appendix). The non-decalcified sample was sectioned into a 400- μm series of slices (Donath and Breuner, 1982), and GFP-labeled SPDs were observed by fluorescence microscopy (Olympus BX/TF, U-LH100HG, Tokyo, Japan). For pair-wise comparison, data were analyzed by one-way ANOVA and the Bonferroni method.

RESULTS

Isolation and Characterization of SPDs

In culture, SPDs form adherent clonogenic cell clusters of fibroblast-like cells, similar to the morphology described in SHEDs; approximately 67 single colonies were generated from 10^5 single cells cultured at low cell density. These colony-forming cells were spindle-shaped (Fig. 1A) and positively stained for STRO-1, vimentin, and ALP (Figs. 1B-1D). Flow cytometric analysis showed an average of 10.9% of SPDs positive for STRO-1 and 21.1% positive for ALP (Figs. 1G, 1H), suggesting a heterogeneous population of cells, as previously reported in other post-natal mesenchymal stem cells, including bone marrow (Shi and Gronthos, 2003), dental pulp (Gronthos *et al.*, 2000), and periodontal ligament stem cells (Seo *et al.*, 2004).

Expression of eGFP Gene and Fabrication of an SPD-Scaffold Construct

The retroviral transfection was carried out on day 2 in culture, followed by a repeated transfection on day 3. Subsequently, transfected SPDs were selected with G418 (100 $\mu\text{g}/\text{mL}$), and colonies expressing green fluorescence were expanded in growth medium (Fig. 1E). After several passages, the progenies of GFP-positive SPDs continued to express eGFP.

For fabrication of the cell-scaffold construct, approximately 2×10^7 - 4×10^8 GFP-positive SPDs at third and fourth passages were seeded onto β -TCP scaffolds and cultured in growth medium for 7 days *in vitro*. SEM studies showed that GFP⁺-SPDs were able to grow on β -TCP scaffolds (Fig. 1F).

SPD-mediated Bone Regeneration in the Reconstructed Mandibular Defect

At 24 wks, animals were killed, and the mandibles were harvested for CT, gross morphology, and histological analyses (Fig. 2, Appendix Fig. 2). CT scan analyses showed nearly complete regeneration of initial defect sites, with new bone formation in the SPD/ β -TCP treatment group as shown in coronal (Fig. 2A) and axial sections (Appendix Fig. 2A), three-dimensional view (Appendix Fig. 2B), as well as gross bone morphology of a sagittal bone section (Appendix Fig. 2C). Histological sections of the SPD/ β -TCP grafted site revealed newly formed lamellar bone and degraded β -TCP scaffold (Fig. 2B). In contrast, in the β -TCP group, the defect site was only partially restored, with significant remaining defect in the lateral cortex of the mandible (Fig. 2C, Appendix Figs. 2D, 2E, and 2F). Histologically, the scaffold-treated defect was partially filled with some new bone formation, connective tissues, and degraded β -TCP (Fig. 2D). In the control, or untreated, group, a marked bone defect remained with predominantly connective tissues (Figs. 2E, 2F). The regenerated defect site displayed a mean of 83.1% of mineralized matrix in the SPD/ β -TCP-treated group, significantly higher than the 52.2% in the scaffold group ($P < 0.01$), and 28.4% higher than in the control group ($P < 0.01$) (Fig. 2G).

At 4 wks post-transplantation, CT scan revealed partial bridging of the lateral cortical continuity defect and moderate bone regeneration in the SPD/ β -TCP-treated group, in conjunction with early scaffold degradation (Fig. 3A). The gross view of the reconstructed defect site displayed marked absorption of scaffold at the junction of native bone and graft in the SPD/ β -TCP-treated group at the early stage of bone healing (Appendix Fig. 3B). Relatively intact scaffold was observed in the β -TCP group (Appendix Fig. 3C), and a large bony defect remained in the untreated group (Appendix Fig. 3D). Histological sections of decalcified specimens showed abundant new islands of bone and blood vessels amid degraded scaffold in the SPD-treated group at 4 wks post-reconstruction (Figs. 3B, 3C). In contrast, in the β -TCP group, the

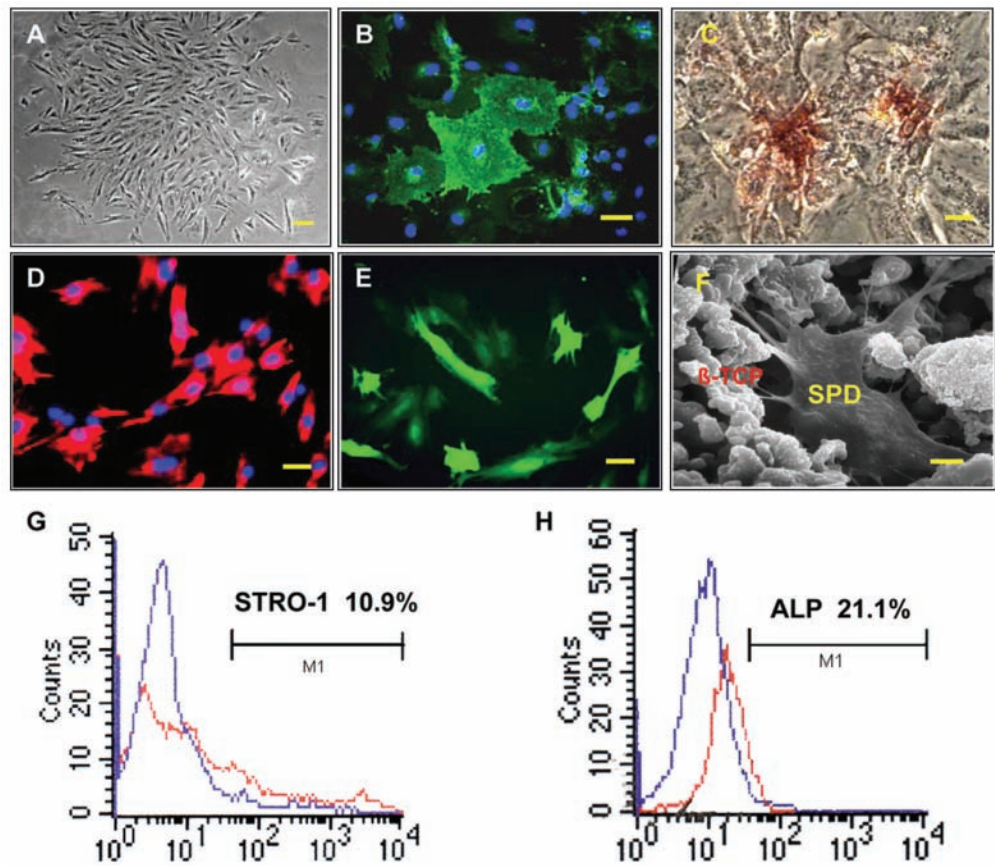


Figure 1. Characterization of stem cells derived from miniature pig deciduous teeth (SPD). (A) Single colonies of SPD showed typical fibroblast-like morphology under light microscopy. (B) SPDs expressed STRO-1 by immunohistochemical staining with anti-STRO-1 antibody and (C) ALP-positive staining with the alkaline phosphatase detection kit under light microscopy. (D) Immunohistochemical staining with anti-vimentin antibody showed 99.5% positive staining. (E) GFP-expressed SPDs showed fibroblast-like morphology. (F) Scanning electron microscopy revealed GFP-labeled SPDs grown on β -TCP scaffold. (G-H) An average of 10.9% of the 3rd-passage SPDs were positively stained for STRO-1 (G) and 21.1% for ALP by flow cytometric analysis (H). Abbreviations: SPD, stem cells from pig deciduous teeth; ALP, alkaline phosphatase. Scale bars: 100 μ m in A; 30 μ m in B, C, D, E; 4 μ m in F.

lateral cortical rim defect remained, with minimal β -TCP absorption (Fig. 3D). The bone void at the defect site remained unfilled in the control group (Fig. 3G, Appendix Fig. 3D). Histological sections showed a lack of new bone formation at the junction of β -TCP scaffold (Figs. 3E, 3F) and abundant connective tissue proper in the untreated group (Figs. 3H, 3I). These findings demonstrated that bone regeneration was significantly higher in the SPD/ β -TCP-treated group as compared with the β -TCP group. In the blank (control) group, limited bone regeneration was observed in the defect area, which was filled predominantly with connective tissue proper (Figs. 3G, 3H, 3I, Appendix Fig. 4D).

Detection of Transplanted GFP-positive SPD in Regenerative Bone

To identify if the GFP-positive SPDs engrafted at the transplanted bone defect sites had differentiated into osteoblasts, we first screened non-decalcified sections using light microscopy for location of osteoblasts and bone lacunae in the new bone at 2 wks and

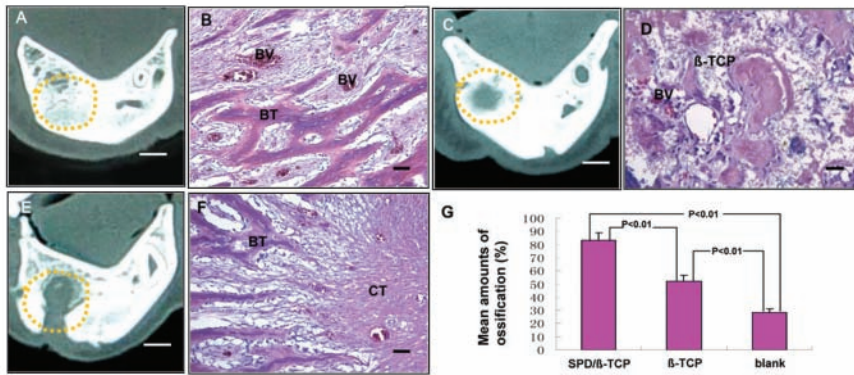


Figure 2. SPD-mediated bone regeneration of critical-size mandibular defect at long-term follow-up. **(A, B)** SPD/ β -TCP-treated group: CT coronal image showed a large quantity of new bone formation filling the bone defect at 24 wks post-transplantation; yellow dot area indicates the original site of the bone defect (A); the histological section shows that the defect was filled with new bone (B). **(C, D)** β -TCP-treated group: CT coronal image shows remaining smaller bone defect at the reconstructed defect site; histological section shows that the defect was partially filled with connective tissues, β -TCP scaffold, and new bone formation (D). **(E, F)** Untreated, or control, group: CT coronal image shows limited bone regeneration and large bone defect remaining; histological section shows that the defect was filled primarily with connective tissues. **(G)** Semi-quantitative analysis of bone formation showed a statistically significant increase in mineralized matrix formation at the regenerated defect site, $83.1 \pm 5.75\%$ (mean \pm SD, $n = 4$) in the SPD/ β -TCP treated group, compared with $52.2 \pm 4.54\%$ ($n = 3$) in the scaffold group ($P < 0.01$), and $28.4 \pm 2.79\%$ ($n = 3$) in the control group ($P < 0.01$). Scale bars: 1 cm in A, C, E; 50 μ m in B, F; 30 μ m in D. BT, bone tissue; BV, blood vessel; CT, connective tissue.

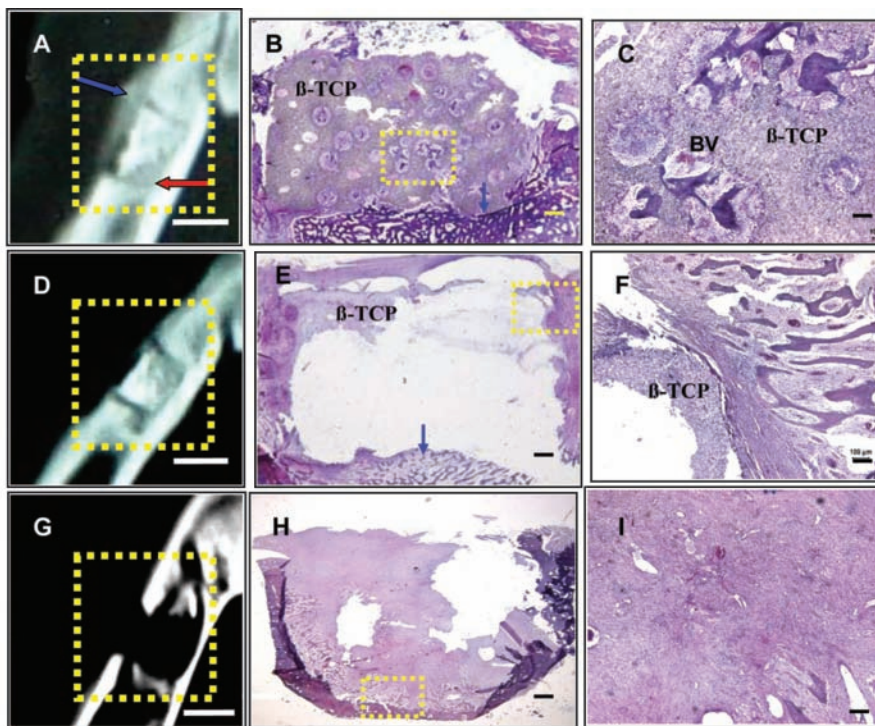


Figure 3. SPD-mediated bone regeneration of small-size mandibular defect at the short-term (wks) follow-up. **(A, B, C)** SPD/ β -TCP-treated group: CT axial image showing replacement of β -TCP scaffold with new bone restoration (red arrow), and bridging of the lateral cortical defect with new bone formation (blue arrow). H&E stain of the regenerated defect site at 10X (B) and 40X (C) revealed several new islands of bones and blood vessels amid degraded scaffold. **(D, E, F)** β -TCP-treated group: CT axial scan showing a partial bridging of the cortical defect and no visible bone formation; H&E stains (E, F) showing sparse new bone formation at the junction of β -TCP scaffold and partially degraded β -TCP. **(G, H, I)** Untreated, or control, group: CT axial scan showing a continuity defect in the lateral cortex and lack of bone regeneration. Histological sections show primarily connective tissues filling the defect of the control group (H and I). Scale bars: 1 cm in A, D, G; 1 mm in B, E, H; 100 μ m in C, F, I. BT, bone tissue; BV, blood vessel; CT, connective tissue.

4 wks post-operatively (Figs. 4A-4D). Using the same visual field, we captured GFP expressing SPDs under a fluorescence microscope (Figs. 4B, 4D). When both images in Figs. 4C and 4D were overlaid, the locations of some GFP-positive SPDs were superimposed with the osteoblasts and bone lacunae (Fig. 4E, yellow arrows showing GFP-negative osteoblasts, red arrows showing GFP-positive osteoblasts), suggesting that GFP-positive SPD cells might have differentiated to osteoblasts. As expected, the normal bone tissue section showed a uniformly distributed green fluorescence signal without local accumulation of GFP-positive cells under immunofluorescence microscopy (Fig. 4F).

DISCUSSION

Craniofacial tissue engineering by stem cells is a fast-moving field with considerable potential clinical applications (Mao *et al.*, 2006; Kaigler *et al.*, 2006; Zhao *et al.*, 2007). Deciduous tooth stem cells are an easily accessible stem cell source and capable of robust *ex vivo* expansion for several potential clinical applications (Miura *et al.*, 2003; Mao *et al.*, 2006; Seo *et al.*, 2008). Embryologically derived from the neural crest cell, SHEDs and SPDs may share similar tissue origin with the mandibular bone cells, and therefore, may serve as a better cell source for the regeneration of alveolar and orofacial bone defects. A previous study showed that the bone-regenerative capacity of SHEDs was similar to that of bone marrow mesenchymal stem cells (BMMSC) when transplanted into immunocompromised mice at 8 wks post-transplantation (33% mineralized matrix/area in the SHED group vs. 31% mineralized matrix/area in the BMMSC group) (Seo *et al.*, 2008). Similar to SHEDs and other post-natal mesenchymal stem cells derived from bone marrow (Shi and Gronthos, 2003), dental pulp (Gronthos *et al.*, 2000), and periodontal ligament stem cells (Seo *et al.*, 2004), it is not unexpected that the SPDs are a heterogeneous population of cells which, following *ex vivo* cultures, may display different percentages of cells positive for STRO-1, or form mineralized nodules, or be positive for Oil red O under differentiation inductive conditions.

In this study, to investigate SPD-mediated bone formation *in vivo*, we labeled SPDs with GFP and used SPDs to repair critical-size bone defects in the mandibles in swine. At 2 and 4 wks after transplantation,

green fluorescence signals were detected by fluorescence microscopy within newly formed woven bone. Photomicrographs of the same visual fields confirmed that GFP-labeled SPDs had differentiated directly into new bone, while the normal bone tissue section was non-specifically labeled with green fluorescence. These findings suggested that SPDs were engrafted to some extent at the treated site and contributed to new bone regeneration in the restoration of the bone defect in the swine mandible model. The results of CT scan, gross view, and histological analyses consistently showed that the SPD group had the earliest and strongest capacity of bone regeneration compared with other groups. At 4 wks post-transplantation, β -TCP was partly degraded and was replaced with a large quantity of new bone formation. At 6 mos post-reconstruction, the defects in the SPD group were markedly restored with new bone, while in the β -TCP group and control group, much less bone regeneration and predominantly connective tissue granulation were evident at the defect sites. Further studies to regulate bone regeneration are under way to optimize the transplanted stem cell numbers, scaffolds, and their immediate niche component.

Overall, our study provides the first evidence that SPDs are capable of regenerating critical-size defects in the orofacial bone in a large-animal model, specifically swine, and may potentially serve as an alternative stem-cell-based approach in the reconstruction of alveolar and orofacial bone defects.

ACKNOWLEDGMENTS

This work was supported by grants from the National Basic Research Program of China (No. 2007CB947304), the Beijing Major Scientific Program (D090600700091), the National Natural Science Foundation of China (Grants 30428009 and 30801297), and the US National Institutes of Health (NIDCR R01DE17449 to S.S.).

REFERENCES

Akintoye SO, Lam T, Shi S, Brahim J, Collins MT, Robey PG (2006). Skeletal site-specific characterization of orofacial and iliac crest human bone marrow stromal cells in same individuals. *Bone* 38:758-768.

Bianco P, Riminucci M, Gronthos S, Robey PG (2001). Bone marrow stromal stem cells: Nature, biology, and potential applications. *Stem Cells* 19:180-192.

Brazelton TR, Blau HM (2005). Optimizing techniques for tracking transplanted stem cells in vivo. *Stem Cells* 23:1251-1265.

Donath K, Breuner G (1982). A method for the study of undecalcified bones and teeth with attached soft tissues. The Sage-Schliff (sawing and grinding) technique. *J Oral Pathol* 11:318-326.

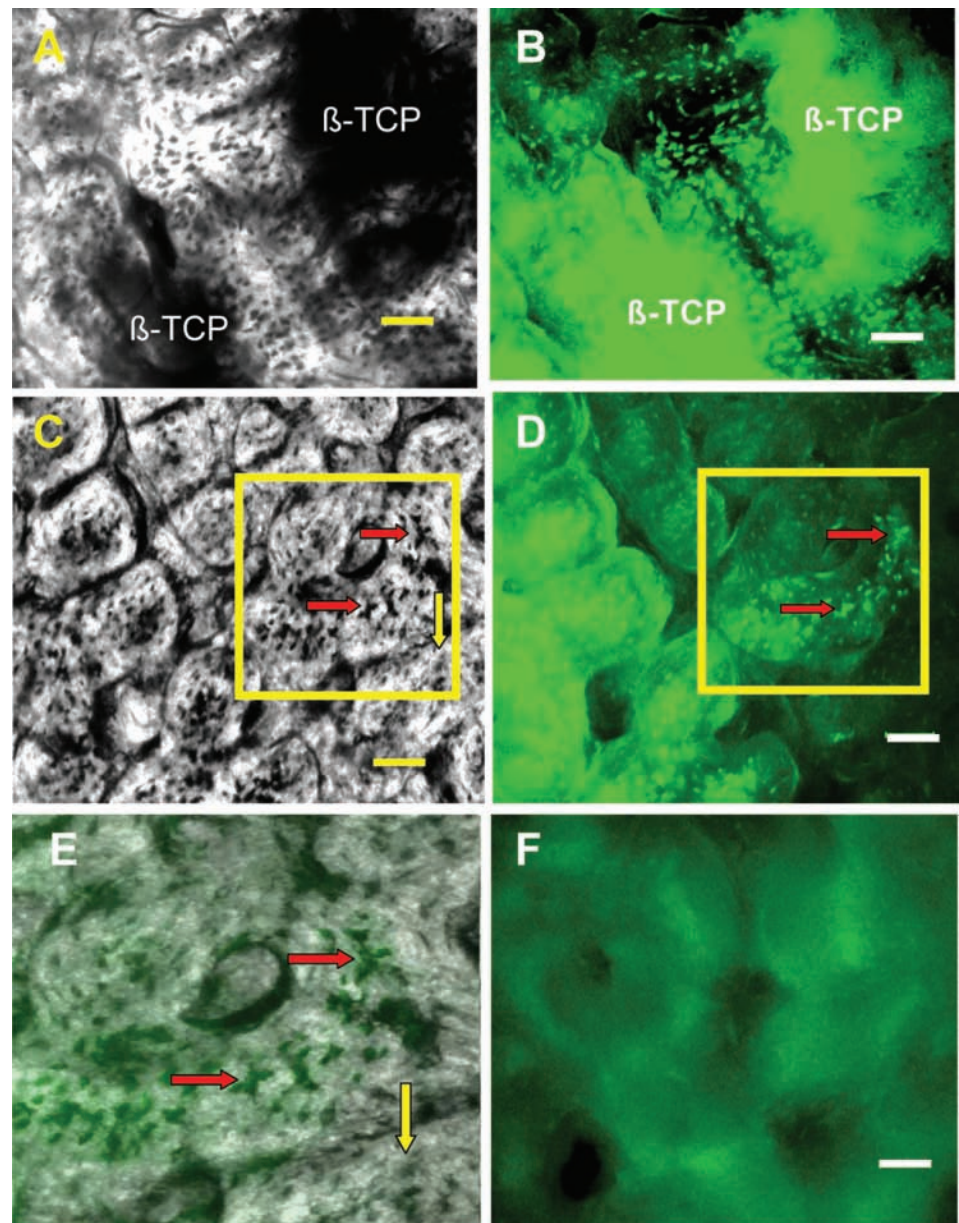


Figure 4. Tracking GFP-labeled SPD in new bone tissue regeneration by immunofluorescence microscopy. **(A, B)** Tracking GFP-positive cells at 2 wks post-transplantation. Trabecular bone/bone lacunae and β -TCP scaffold in the restored defect area were observed under light microscopy (A). In the same visual field, the cells from newly formed bone tissue and β -TCP scaffold area were screened for GFP-labeled SPD by fluorescence microscopy (B). **(C, D, E)** Tracking GFP-positive cells at 4 wks post-transplantation. New trabecular bone and lacunae were observed in the defect area (C). In the same visual field, the cells in newly regenerated bone tissue were shown to express GFP label by fluorescence microscopy (D). When Figs. 4C and 4D were overlaid, the locations of some GFP-positive SPDs were superimposed within the area of bone lacunae (yellow arrow shows GFP-negative bone cells, red arrows show GFP-positive bone cells), suggesting that new immature bone tissues may be derived from both GFP-labeled SPDs and host osteoblasts. **(F)** Normal bone tissue section of miniature pig's mandible showing non-specific distribution of green fluorescence by immunofluorescence microscopy. Scale bars: 50 μ m.

- Gronthos S, Mankani M, Brahim J, Robey PG, Shi S (2000). Postnatal human dental pulp stem cells (DPSCs) in vitro and in vivo. *Proc Natl Acad Sci USA* 97:13625-13630.
- Gronthos S, Zannettino AC, Hay SJ, Shi S, Graves SE, Kortessidis A, *et al.* (2003). Molecular and cellular characterization of highly purified stromal stem cells derived from human bone marrow. *J Cell Sci* 116(Pt 9):1827-1835.
- Henkel KO, Gerber T, Dorfling P, Gundlach KK, Bienengraber V (2005). Repair of bone defects by applying biomatrices with and without autologous osteoblasts. *J Craniomaxillofac Surg* 33:45-49.
- Kaigler D, Krebsbach PH, Wang Z, West ER, Horger K, Mooney DJ (2006). Transplanted endothelial cells enhance orthotopic bone regeneration. *J Dent Res* 85:633-637.
- Liu Y, Zhang Y, Ding G, Fang DJ, Zhang CM, Shi S, *et al.* (2008). Periodontal ligament stem cells-mediated treatment for periodontitis in miniature swine. *Stem Cells* 26:1065-1073.
- Mankani MH, Kuznetsov SA, Shannon B, Nalla RK, Ritchie RO, Qin Y, *et al.* (2006). Canine cranial reconstruction using autologous bone marrow stromal cells. *Am J Pathol* 168:542-550.
- Mao JJ, Giannobile WV, Helms JA, Hollister SJ, Krebsbach PH, Longaker MT, *et al.* (2006). Craniofacial tissue engineering by stem cells. *J Dent Res* 85:966-979.
- Mastrogiacomo M, Papadimitropoulos A, Cedola A, Peyrin F, Giannoni P, Pearce SG, *et al.* (2007). Engineering of bone using bone marrow stromal cells and a silicon-stabilized tricalcium phosphate bioceramic: evidence for a coupling between bone formation and scaffold resorption. *Biomaterials* 28:1376-1384.
- Miura M, Gronthos S, Zhao M, Lu B, Fisher LW, Robey PG, *et al.* (2003). SHED: stem cells from human exfoliated deciduous teeth. *Proc Natl Acad Sci USA* 100:5807-5812.
- Petite H, Viateau V, Bensaid W, Meunier A, de Pollak C, Bourguignon M, *et al.* (2000). Tissue engineered bone regeneration. *Nat Biotechnol* 18:959-962.
- Rose FR, Oreffo RO (2002). Bone tissue engineering: hope vs hype. *Biochem Biophys Res Commun* 292:1-7.
- Seo BM, Miura M, Gronthos S, Bartold PM, Batouli S, Brahim J, *et al.* (2004). Investigation of multipotent postnatal stem cells from human periodontal ligament. *Lancet* 364:149-155.
- Seo BM, Sonayama W, Yamaza T, Coppe C, Kikuri T, Akiyama K, *et al.* (2008). SHED repair critical-size calvarial defects in mice. *Oral Dis* 14:428-434.
- Shan Z, Li J, Ou G, Liu X, Zhang C, Baum BJ, *et al.* (2005). Structural and functional characteristics of irradiation damage to parotid glands in the miniature pig. *Int J Radiat Oncol Biol Phys* 62:1510-1516.
- Shao X, Goh JC, Huttmacher DW, Lee EH, Zigang G (2006). Repair of large articular osteochondral defects using hybrid scaffolds and bone marrow-derived mesenchymal stem cells in a rabbit model. *Tissue Eng* 12: 1539-1551.
- Shi S, Gronthos S (2003). Perivascular niche of postnatal mesenchymal stem cells in human bone marrow and dental pulp. *J Bone Miner Res* 18:696-704.
- Shi S, Gronthos S, Chen S, Reddi A, Counter CM, Robey PG, *et al.* (2002). Bone formation by human postnatal bone marrow stromal stem cells is enhanced by telomerase expression. *Nat Biotechnol* 20:587-591.
- Sonoyama W, Liu Y, Fang D, Yamaza T, Seo BM, Zhang C, *et al.* (2006). Mesenchymal stem cell-mediated functional tooth regeneration in swine. *PLoS ONE* 1:e79.
- Wang SL, Liu Y, Fang DJ, Shi ST (2007). The miniature pig: a useful large animal model for dental and orofacial research. *Oral Dis* 13:530-537.
- Yan X, Voutetakis A, Zheng C, Hai B, Zhang CM, Baum BJ, *et al.* (2007). Sorting of transgenic secretory proteins in miniature pig parotid glands following adenoviral mediated gene transfer. *J Gene Med* 9:779-787; *erratum in J Gene Med* 9:1106, 2007.
- Zhang H, Zhao Y, Zhao C, Yu S, Duan D, Xu Q (2005). Long-term expansion of human neural progenitor cells by epigenetic stimulation in vitro. *Neurosci Res* 51:157-165.
- Zhao Z, Wang Z, Ge C, Krebsbach P, Franceschi RT (2007). Healing cranial defects with AdRunx2-transduced marrow stromal cells. *J Dent Res* 86:1207-1211.